EVALUATION OF MICROMECHANICAL PROPERTIES OF *NEUROPELTIS ACUMINATAS* (NA) FIBERS

F. Betene Ebanda[1], Y.S. Nnengue Evoung[1], J. Atangana Ateba[1], J.B. Saha Tchinda[3,4], A.M. Tcheumani Yona[3], Tawe Laynde[2]

[1]Laboratory of Mechanics and Production, University of Douala
[2]Laboratory of Mechanics and Civil Engineering, University of Maroua
[3]Laboratory of Macromolecular Chemistry, University of Yaounde 1, BP 812, Yaounde
CAMEROON
[4]Laboratory of Studies and Research on Wood Material (LERMAB), Faculty of Science and Technology, University de Lorraine, EA 4370 USC INRA, BP 70239, F-54506 Vandoeuvre lès Nancy
FRANCE
Corresponding Author Email : yannick.nnengue@yahoo.com

ABSTRACT

The present work aims at determining the chemical composition as well as the micromechanical properties of the fibers coming from a liana of South Cameroon locally called "Ndik Kussa" of scientific name Neuropeltis acuminatas (NA). After obtaining NA fibers by a traditional method, spectroscopic spectroscopic analysis at the spectograph of the fiber reveals the presence of the H-O groups of the polysaccarides and the water of hydration, the C-H groups of the cellulose, the groups of the esters and acids of hemicelluloses, $C=C$ lignin groups, C-O groups of cellulose, acetyl groups of lignin, C-H groups and aromatic vibrations, CH_2 groups of polysaccharides. A tensile test is performed on ten fibers of 90mm length. The degree of crystallinity is calculated by the method of Segal. A relation between elongation at the beginning of the linear zone and the angle of the microfibrils is established, leading to the deduction of the mirofibrillar angle. Thus, with the relation based on isochoric deformations, a relation between the Young's modulus of the crystalline and noncrystalline parts of the fiber is established, making it possible to have an evolution of the Young's modulus of the crystalline and noncrystalline parts. The results indicate that the cellulose microfibrils are oriented $1,39°$ with respect to the axis of the fiber. They also reveal that the crystallinity index is $CrI(\%)=42$ and that the Young's modulus of the crystalline and non-crystalline parts evolves according to a linear law.

Key words: *Neuropeltis acuminatas*, fiber, micromechanical properties, chemical composition.

1. INTRODUCTION

The exploitation of renewable resources is an essential concern today for the preservation of the environment. Developing countries, including those in sub-Saharan Africa, are seizing this opportunity to exploit local resources that are still unexplored. An ideal example is the physical exploitation of secondary agricultural products, such as the fibers of the banana plant [1], [2].
In fact, cellulosic fibers extracted from plant fibers seem particularly suitable for polymers for the purpose of reinforcement: actually, the vegetable fibers most frequently used in composites are extracted from liberian fibers. This consumes for example jute, flax and hemp, hard fibers, which are quite well exploited industrially. As far as agricultural waste is concerned, the stems of herbaceous plants may be used for this purpose, although these plants are less often used for fiber extraction by traditional retting. Examples of fibers extracted from herbaceous plants that have been proposed for use in materials include, for example, switchgrass, alfalfa, celery and nettle, but in some cases more as agro-waste loads than as semi-structural [3].The implementation of new materials from renewable natural resources is essential for both environmental and economic reasons [4]. Nowadays, great attention and interest is given to experimenting with natural fibers to replace synthetic fibers [5].

The use of natural fibers in polymer composites to replace synthetic fibers such as glass is receiving increasing attention because of their abundance, their renewable character, their high rigidity, their non-abrasion of the treatment equipment, the possibility of their incineration. Thus, cellulose nanofibers have been tested to strengthen different polymeric matrices such as starch [6]; [7] ; [8], polyvinyl alcohol [9] ; [10], polylactic acid [11]; [12] ; [13]; [14] ; [15] ; [16] ; [17] and other polymers [18] ; [19] ; [20].

Neuropeltis acuminatas is a woody vine with twisted stems up to 40 m long and up to 25 cm in diameter. It has alternate, simple leaves with petioles 8-25 mm long; The lamina is elliptical, 5-12 cm × 5-6 cm, rounded to wedge-shaped at the base, having an entire margin. This liana has inflorescence with axillary and terminal clusters, up to 50 flowers, 12-30 cm long [21]. Its flowers are bisexual, regular, fragrant; The pedicels are 4 mm long, bracts strongly accrescent after flowering [22]; The sepals are circular to elliptical, 1.5-3 mm long and pubescent. Its fruit is a rounded capsule 7 mm in diameter, surrounded at the base by the persistent calyx and dilated bract [23]. Its seeds are globose, black, glabrous [5].NA fibers have since been used by our ancestors in South Cameroon. These formed a pile of fibers that they used as a dish sponge and toilet gang.

The present work consists in evaluating the chemical composition and the micromechanical characteristics of the new fiber. It is a question of determining its crystallinity rate, the angle of its microfibrils, identifying the internal chemical groups, and evaluating the range of values of the Young's modulus of its cellulosic and amorphous parts.

2. MATERIALS AND METHODS

2.1 Materials

2.1.1. Diffractometer

This evaluation is carried out by diffractogram, The Philips X'Pert Pro diffractometer with a CuKα radiation, (λ = 1.5405980 Å) and steps of 0.0001 ° is used. The monochromator is graphite and has a voltage of 45 KV.The Segal method used here is very common and easy to implement and remains the most used for determining the crystallinity index of natural cellulosic fibers [24]; [25].

2.1.2. Traction test

The traction test is performed on an INSTRON version IX2716-010 machine type 004 with a PC interface for automatic acquisition of forces and displacements. Individual fiber test pieces of NA are made by providing both ends of mooring heads. Between the two mooring heads a free length of 90 mm is left. Traction tests are carried out on 14 specimens at a speed of 20 mm / min [26].

2.1.3. Chemical composition

The chemical characterization will require an oven, a thermostatic oven, an electronic scale, a desiccator, a heated flask, a cooling device, a No 4 crucible.

2.1.4. Infrared spectrography

It is made by infrared spectrography. The spectrograph used is of BRUCKER Alpha model of resolution4 cm^{-1}, with a scan number equal to 24.

2.2 Method

2.2.1 Evaluation of the angle of the microfibrils

The tensile characterization of the fiber has been the subject of an earlier article [27]. It is a question of exploiting the results of said characterization to determine the microfibrillar angle. Figure 1 is a simplified representation of the microfibrils of celluloses.
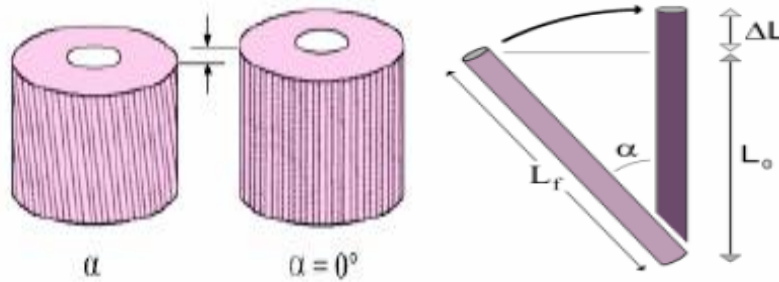
Figure 1: Simplified representation of the orientation of cellulose microfibrils [28]

The value of L_0, is obtained in the following way:

$$L_0 = L_f cos\alpha$$

Where L_f is length of a microfibrillary,
         L_0 projection along the axis of the fiber

From this value, ΔL is calculated as follows:

$$\Delta L = L_f - L_0 \Rightarrow \Delta L = L_0 \left(\frac{1}{cos\alpha} - 1\right) \qquad (2)$$

Where ΔL is lengthening the fiber

Let the global deformation of:

$$\mathcal{E} = ln\left(1 + \frac{\Delta L}{L_0}\right) = -ln(cos\alpha) \qquad (3)$$

Where $\mathcal{E}$ Global deformation

The determination of the angle corresponding to a given deformation can therefore be obtained by the equation [28]:

$$\alpha = Arc\,cos(e^{-\mathcal{E}}) \qquad (4)$$

The deformation at the beginning of the linear zone of the stress-strain curve is taken and the relation $\alpha = Arc\,cos(e^{-\mathcal{E}})$ between the microfibrillar angle α and the strain $\mathcal{E}$ at the beginning of the linear zone is applied.

2.2.2. Young's modulus of crystalline and non-crystalline parts

Microscopic modeling of the Young's modulus is made from the crystallinity index, the microfibrillar angle and the Young's modulus of the fiber obtained during the tensile characterization.

The equation of isochoric deformation, which describes the behavior of the low-helix fibril disclosed by Thygesen et al., in 2005, made it possible to determine a relationship between the longitudinal Young's modulus of the crystalline parts as a function of the modulus of Young non-crystalline parts. This relationship is given by equation 5 described below:

$$E_1 = [X_{1C}E_{1C} + (1 - X_{1C})E_{NC}]cos^2X_2 = E\ cos^2X_2 \qquad (5)$$

Where E_1 is longitudinal elasticity modulus of the fiber,

E_{NC} Young's modulus of non-crystalline parts

X_2 propeller angle

X_{1C} content of the crystalline parts

E Young module of NA fiber.

2.2.3. Chemical characterization

Extraction methods with alcohol-benzene

A cartridge containing a mass of 14 g of fibers milled in a Retsch SM 100 mill with a blade. The volume ratio of ethanol-benzene ½ (500 ml of benzene and 250 ml of ethanol). The mixture is introduced into a flask; this flask is heated and a soxhlet is introduced and is closed with a coolant for 8H of time; The solid residue is washed with distilled water, then heated in a thermostatic oven at 150 ° C overnight and then weighed, the level of alcohol-benzene extract is obtained by the following equation [29] 6:

$$E_{AB} = \frac{m_{AB}}{m_E}x100 \qquad (6)$$

Where E_{AB} is Percentage of ethanol-benzene extract,

m_{AB} mass of the residue dried at 105 ° C in a thermostatic oven

m_E mass of the sample taken for the experiment.

Methods of extraction with water

1.5 g of sawdust and 100 ml of distilled water are introduced into a ground-necked Erlenmeyer flask and boiled under reflux with magnetic stirring for 7 hours. The solid residue is washed with distilled water, then heated in a thermostatic oven at 150 ° C overnight and weighed. The rate of extract with water is obtained by the following equation [29] 7:

$$E_e = \frac{m_{fs}-m_{se}}{m_{fs}}\left(100 - E_{AB}\right) \qquad (7)$$

Where E_e is percentage of water,

m_{fs} dried fiber mass for the experiment

m_{se} mass of dry fibers exiting the thermostatic oven after the experiment.

Method for Lignin Rate (KLASON Method)

300 mg of sawdust extracted with ethanol-benzene and water are introduced into 5 ml of 72% sulfuric acid for 1H, 195 ml of water are added to the mixture and refluxed during 4H, then filtered with a crucible N° 4 for 4H. The solid residue is washed with distilled water, then heated in an oven at 150 ° C overnight and weighed. The lignin level is obtained by the following method [29]:

$$L = \frac{m_L}{m_E}(100 - E_{AB}) \qquad (10)$$

Where L is lignin levels,

     m_L mass of lignin extracted after the experiment.

Method for the rate of pectin

2 g of sawdust extracted with ethanol -benzene and water, having been dried in an oven are introduced into 100 ml of 2% chloridic acid heated at reflux for 4H, then filtered with a crucible No. 4 for 4H. The solid residue is washed with distilled water, then heated in a thermostatic oven at 150 ° C overnight and weighed. The pectin content is obtained by the following method [29] (9):

$$P = \frac{m_P}{m_E}(100 - E_{AB}) \qquad (9)$$

Where P is pectin level

     m_L mass of pectin extracted after the experiment.

Method for Holocellulose Rate

500 mg of extracted sawdust were placed in a 100 mL flask containing 30 mL of distilled water and heated at 75 °C. Acetic acid (0.1 mL) and 15% aqueous sodium chlorite (2 mL) were then added each hour for 7 h. The mixturewas filtered on a Büchner funnel and the residue washed with water, Soxhlet extracted for 2 h with ethanol and dried at 103 °C to a constant mass [29].

Method for the Cellulose Rate (Kurschner)

1.5 g of sawdust and 50 ml of nitro-alcoholic solution (40 ml of alcohol and 10 ml of fuming nitric acid) are introduced into a colander Erlenmeyer connected to a refrigerant and heated in a bain-marie for 1 hour. After three attacks, the contents are rerun on a crucible N ° 4; then the contents are washed with ethanol 96 °, with distilled water and with ether; the crucible is heated in an oven for 2 hours and weighed: The cellulose content is obtained by the following method [29]:

$$C = \frac{m_C}{m_E}(100 - E_{AB}) \qquad (11)$$

Where C is cellulose content,

     m_c mass of cellulose extracted after the experiment.

3. RESULTS AND DISCUSSIONS
3.1. Chemical characterization
3.1.1 Chemical composition of NA fiber

NA fibers (*Neuropeltis acuminatas*) contain 39.2 cellulose, 7.2 hemicellulose, 20.4% lignin, 18.9% pectin, 10.8% fats and waxes and 1.5% water-soluble compounds. The ash ash content at 315 μm is 1.973% and at 500 μm is 2.186%. In Table 1 are reported, with respect to NA fibers, the various chemical compositions of certain Liberian fibers widely used as reinforcement in natural composites. From Table 1, it appears that NA fibers are very rich in lignin compared to several fibers of literature except at Alpha. This rate is twice that of jute, abaca and kenaf fibers, and four times higher than the rate found in banana fibers. The level of pectin is much higher than that of the majority of fibers in the literature. This pectin content is 1.561 times higher than that of Diss. The hemicellulose rate of NA is lower than that of the majority of the fibers present in the literature, it is 1.263 slightly higher than that of cotton.

Table 1 :Chemical composition and moisture content of some bast fibres.

Type of fibers	Cellulose %	Hémicellulose %	Lignine %	Pectine %	References
Hemp	70.2-74.4	17.9-22.4	3.7-5.7	0.9	[30]
Flax	64.1–71.9	16.7–20.6	2.0–2.2	1.8–2.3	[31]
Okra	60–70	15–20	5–10	3.7	[31]
Banana	64	10	5	-	[30]
Abaca	59	-	12.5	-	[30]
Sisal	67-78	10-14.2	8.0-11.0	10	[32]
Raphia	58,5	13,4	26,8	-	[32]
Jute	61.0-71.5	13.6-20.4	12.0-13.0	0.2	[30]
Kenaf	51	21.5	10.5	-	[30]
Pineapple	70-82	-	8-12.7	-	[30]
Alpha	45	24	24	5	[33]
Cotton	85-90	5,7	0,7-1,6	0-1	[33]
Ramie	68.6–76.2	13.1–16.7	0.6–0.7	1.9	[33]
Diss	41.1	27	16.8	12.1	[33]
bamboo	32-44	22	19-24	6-8	[33]
sugar	26-43	15	21-31	9-35	[33]
Date palm	35	28	27	10	[34]
NA	39.2	7.2	20,4	18,9	-

3.1.2. Identified chemical groups

Figure 4 shows the infrared spectrum of the NA fiber.
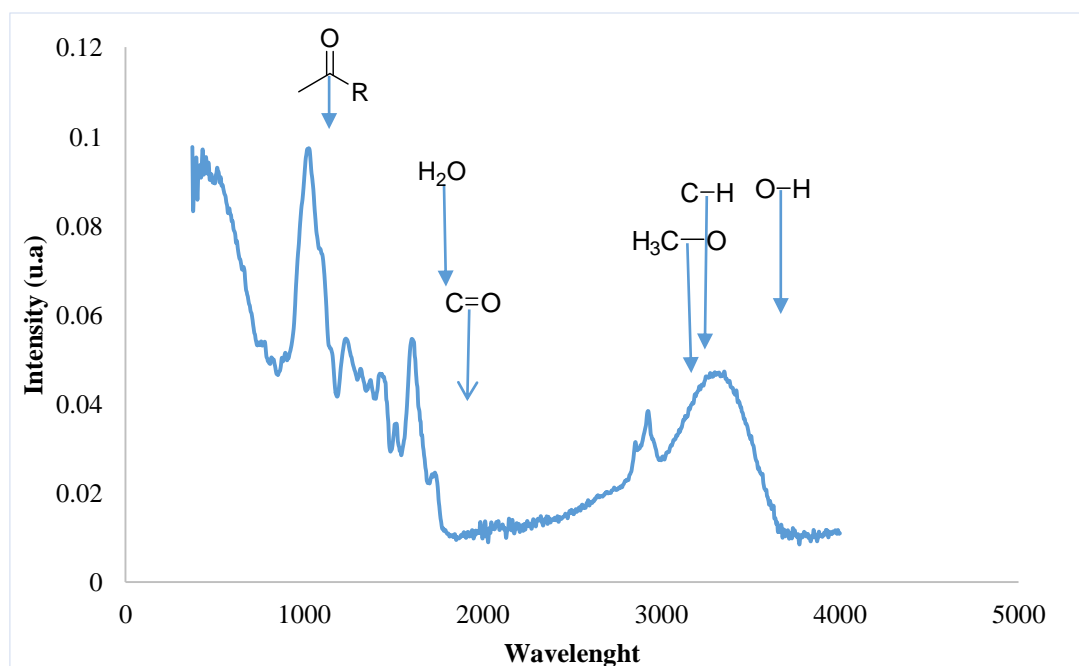
Figure 4: Infrared spectrum of NA fiber

It appears from this figure that the different wavelengths of absorption correspond to that of the fibers regularly studied. Thus the wavelength of 3334 cm $^{-1}$ corresponds to the extensional vibration of the H-O bond of the polysaccharides and the water of hydration. That at 2931 corresponds to the elongation vibration of the C-H bond of the cellulose. That at 2865 corresponding to the symmetrical elongation of the group C=O of esters and acids of hemicelluloses. The length at 1616 corresponds to the hydrogen bonding of the water bound to the fiber. The length at 1519 corresponds to the

symmetrical elongation vibration of the lignin groups $C=C$. That at 1252 corresponds to the vibration of the C-O groups of the cellulose. The length at 1032 corresponds to the deformation of the acetyl groups of the lignin. It should also be noted small peaks at 1454 and 1325. That at 1454 corresponds to the deformation in the plane of C-H groups and aromatic vibrations. That at 1325 corresponds to the deformation in the CH_2 group plane of the polysaccharides. These results are in accordance with those obtained in the literature [35]; [36]; [37].

3.2 Micromechanical characteristics

3.2.1. Microfibrillary angle of NA fiber

By observing the curves $\sigma(\varepsilon)$ in tension, the deformation occurred before the beginning of the linearity of the curve would correspond to the deformation related to the angle of the microfibrils. That is to say that after rapid energization of all the walls of the fiber, the amorphous portion of the fiber would deform elasto-visco-plastic at the same time as the cellulose microfibrils align with the traction axis.
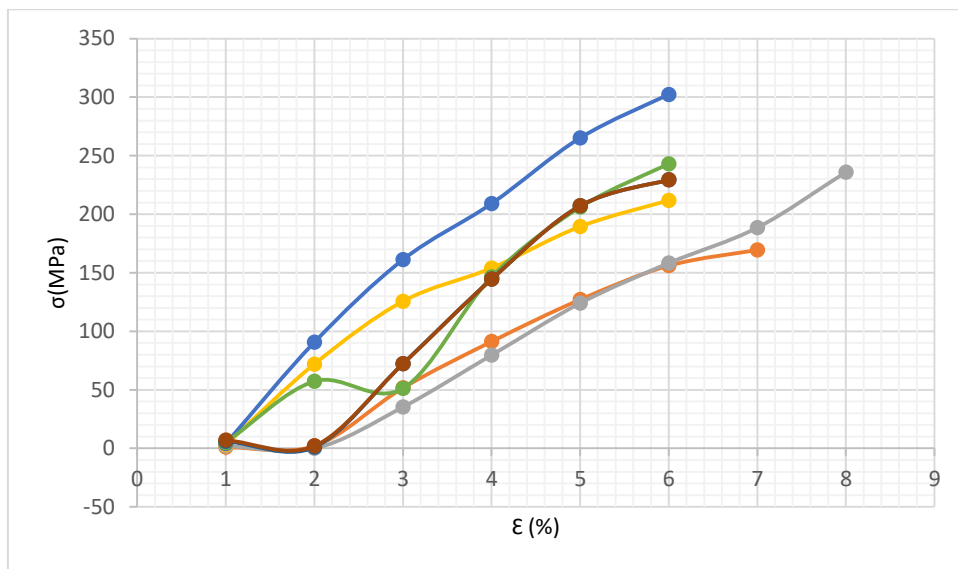
Figure 2: Curves σ (Ɛ) of some NA samples

The following table groups the elongations of the beginning of the linear zone of ten samples.

Table 2: Table of elongations of 10 samples from the beginning of the last linear zone

Samples	Stretching
sample 1	$\varepsilon_1 = 0{,}0373$
sample 2	$\varepsilon_2 = 0{,}0374$
sample 3	$\varepsilon_3 = 0{,}0375$
sample 4	$\varepsilon_4 = 0{,}0358$
sample 5	$\varepsilon_5 = 0{,}02$
sample 6	$\varepsilon_6 = 0{,}0004$
sample 7	$\varepsilon_7 = 0{,}0003$
sample 8	$\varepsilon_8 = 0{,}002$
sample 9	$\varepsilon_9 = 0{,}0007$
sample 10	$\varepsilon_{10} = 0{,}00021$

Figure 3 shows the microfibrillar angle distribution of tested fibers of NA.
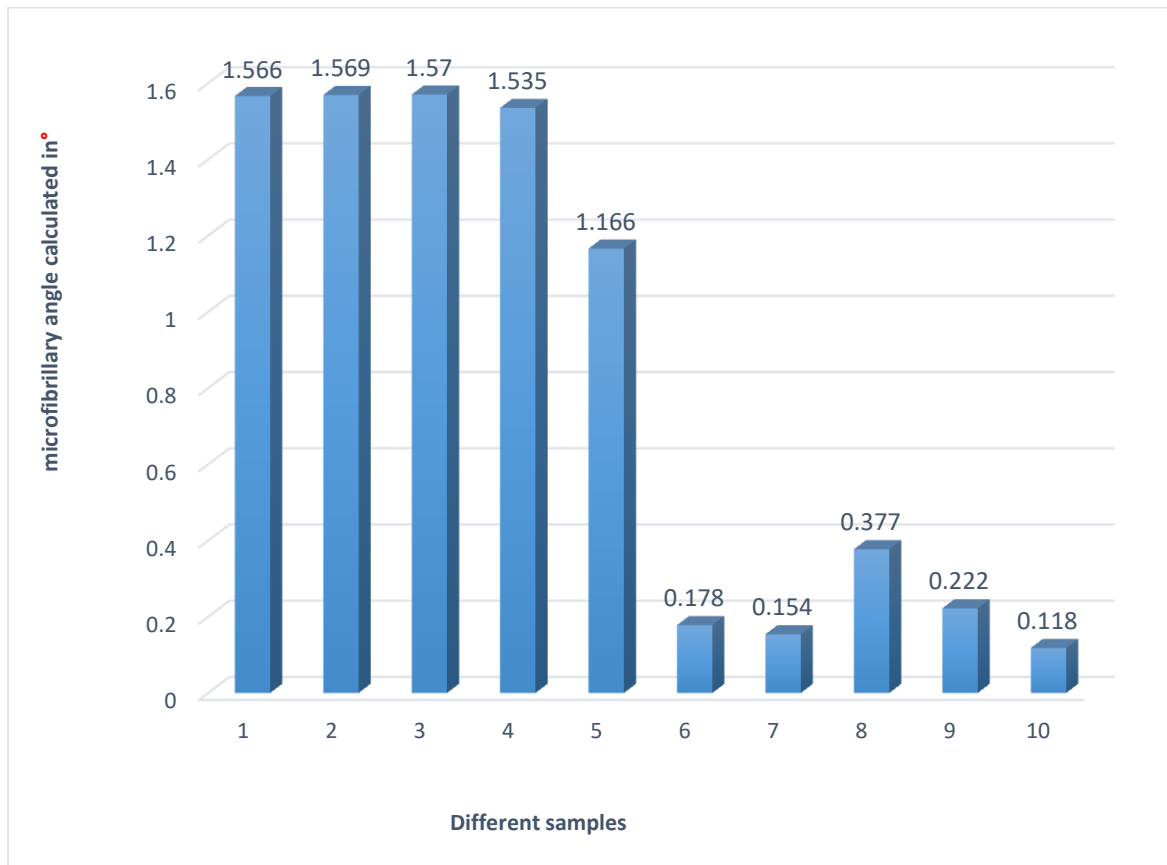
Figure 3: Distribution of microfibrillar angles of NA fibers

In view of these results, it therefore seems that, in a tensile test, the cellulose microfibrils, initially oriented at an average of 1.39 ° of the axis of the fiber, reorganize and progressively align themselves. with the traction axis. This reorganization causes collateral viscoelasto-plastic deformations. By the same calculation method, the angle values of the following fibers were calculated (Table 3).

Table 3: the fibrillated micro angle of certain plant fibers

Fibers	Microfibrillary angle (°)	Elongation (%)	References
Cotton	18,4	7-8	[28]
Hemp	6,9	1.2-3.8	[28]
Ramie	6,4	1.6	[28]
NA	1,39	1.02	-

The angle of inclination of the cellulose microfibrils of NA fiber is lower than that of Ramie fiber, hemp and cotton. In view of the very low inclination of the cellulose microfibrils, they reorganize and align more quickly than the three previous fibers when they are subjected to a tensile force. This explains why the elongations during the tensile test of NA fibers are very low compared to most plant fibers.

3.2.2 Crystallinity index of NA fiber

In Figure 5 is presented the diffractogram of NA fiber.
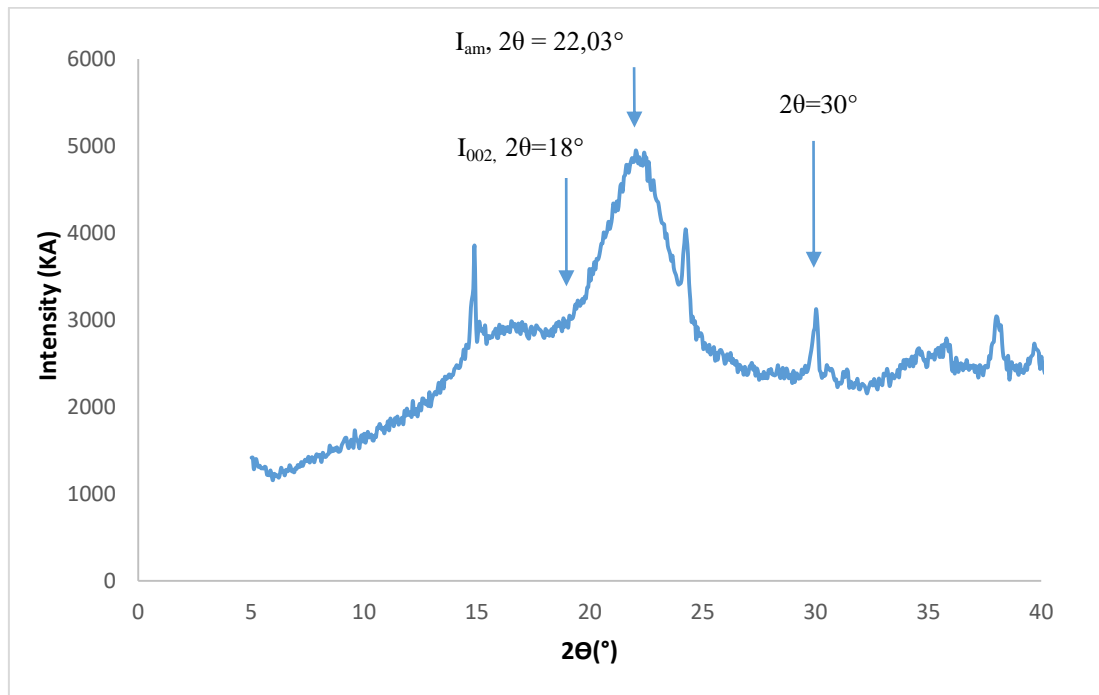
Figure 5: The diffractogram of NA fiber

It appears that this diffratogram has four characteristic peaks which indicate the semi-crystallinity of the fiber, with a very pronounced peak around $2\theta = 21$ °. The major ($2\theta = 21$ °) and low ($2\theta = 30$ °) crystalline peaks can be attributed to the monoclinic structure of crystalline cellulose. The crystalline peak lying around $2\theta = 18$ ° can be attributed to the low crystallinity of crystalline cellulose I. This low crystallinity is explained by the fact that the fiber contains a fairly high level of amorphous materials (we have a fairly high lignin content of the order of 20.4%). In conclusion note: NA fiber has a low degree of crystallinity. These results are confirmed by the results obtained in IR. The wavelength obtained at 1616 cm $^{-1}$, which is attributed to the vibration of the hydrogen bonds of water adsorbed by crystalline cellulose, is therefore not surprising in the case where the cellulose has a low crystallinity, so the active surface is exposed to hydration [38]. After this analysis, the determination of the crystallinity index of the NA fiber will be done using a very usual method which is that of Segal et al., 1959.

This index CrI (%), is determined from equation (1), using the intensities of the lines 002 (I_{002}, $2\theta = 18$ °), and 110 (I_{am}, $2\theta = 22.03$ °). I_{002}, represents both the contribution of the amorphous and crystalline part of the material whereas I_{am} represents only the amorphous part contribution of the material. This method assumes that the contribution of the amorphous portion is the same for the angles at 18 ° and 22.03 °, and that the crystalline cellulose does not contribute to the diffracted intensity at 18 ° [39]. This determination of the crystallinity index remains questionable, however, since it takes into account only the intensities of the lines and not the integrated intensity of the diffraction peaks. However, this method is widely used and described in many studies [24]; [25]. The crystallinity index of NA fiber was calculated using equation 12 below:

$$CrI(\%) = \frac{I_{002} - I_{am}}{I_{002}} \times 100 = \frac{4946 - 28,73}{4946} \times 100 = 42 \qquad (12)$$

Where CrI(%) is crystallinity rate,

I_{002} intensity of the crystalline phase at $2\theta = 5,073°$

I_{am} intensity of crystalline phase at $2\theta = 5,230°$

In table 4 are reported in comparison with the NA, the crystallinity indices of some plant fibers calculated according to the method of Segal.

Table 4: Crystalline indices of certain plant fibers..

Vegetale Fibres	CrI (%)	E (GPa)	σ (MPa)	References
Cotton	86	5.5-12.6	287-597	[40]
Ramie	92	61.4-12.8	400-938	[40]
Hemp	81	35	389	[41]
NA	42	6.043	61.64	-

From this table, it appears that the crystallinity index of the NA fiber is lower respectively than that of the date palm, hemp, cotton and ramie. The glance of the chemical properties, in which the NA has more amorphous material makes it possible to support this analysis. It is therefore normal that the mechanical properties of the NA fiber are low compared to the majority of plant fibers, in that it is the cellulosic materials which contain the cellulose microfibrils and which act as reinforcement in the microstructure. Fiber, which results in the fact that this fiber has low stresses at break.

3.2.3 Young longitudinal module of the crystalline and non-crystalline parts

Taking into account the numerical values, $X_{1C}=CrI(\%)=42$, $X_2 = \alpha = 1,39°$ and $E = 6.043$ Mpa [27], the equation (5) becomes:

$$X_{1C}E_{1C} + (1 - X_{1C})E_{NC} = \frac{E_1}{cos^2 X_2} \Rightarrow E_{1C} + \frac{(1-42)}{42}E_{NC} = \frac{6.043}{42cos^2 1,39}$$

$$\Rightarrow E_{1C} = 0.976E_{NC} + 0.144 \qquad (13)$$

The following figure 6 is the graphical representation of the straight line (13), which is the relationship between the longitudinal Young's modulus of the crystalline and non-crystalline parts.
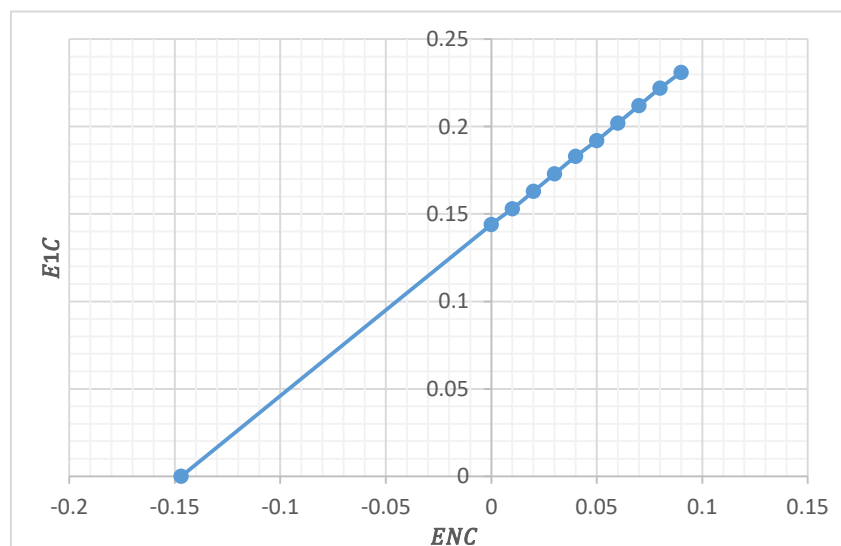
Figure 6: The graphical representation of the evolution of the longitudinal Young's modulus of the crystalline and non-crystalline parts

In this figure, it appears that the longitudinal Young's modulus of the crystalline and non-crystalline parts has a linear progression. Assuming the non-existence of the non-crystalline parts, the minimum Young's modulus of the crystalline parts is: $E_{1c\ min} = 0.144$.

CONCLUSION

The crystallinity index of the NA fiber is *CrI* (%)=42. This crystallinity index is lower respectively than that of the date palm, hemp, cotton and ramie. The finding is clear, the NA contains less cellulosic material than these plant fibers. The breaking stress of the NA fiber is low because it has fewer cellulosic materials that act as reinforcement opposing the forces that are submitted to it. The angle of inclination of the cellulose microfibrils of NA fiber is lower than that of the Ramie fiber, hemp and cotton. In view of the very low inclination of the cellulose microfibrils, they reorganize and align more quickly than the three previous fibers when they are subjected to a tensile force. This explains why the elongations during the tensile test of NA fibers are very low compared to most plant fibers. The infrared analysis of the fiber made it possible to highlight the presence of the HO groups of the polysaccharides and the water of hydration, the CH groups of the cellulose, the groups of the esters and acids of the hemicelluloses, the groups $C=C$ of the lignin, CO groups of cellulose, acetyl groups of lignin, CH groups and aromatic vibrations, CH_2 groups of polysaccharides. The Young's modulus of crystalline parts and non-crystalline parts evolves according to a linear law. The crystallinity index of the NA fiber is *CrI* (%)=42. This crystallinity index is lower respectively than that of the date palm, hemp, cotton and ramie. The finding is clear, the NA contains less cellulosic material than these plant fibers. The breaking stress of the NA fiber is low because it has fewer cellulosic materials that act as reinforcement opposing the forces that are submitted to it. The angle of inclination of the cellulose microfibrils of NA fiber is lower than that of the Ramie fiber, hemp and cotton. In view of the very low inclination of the cellulose microfibrils, they reorganize and align more quickly than the three previous fibers when they are subjected to a tensile force. This explains why the elongations during the tensile test of NA fibers are very low compared to most plant fibers. The infrared analysis of the fiber made it possible to highlight the presence of the HO groups of the polysaccharides and the water of hydration, the CH groups of the cellulose, the groups of the esters and acids of the hemicelluloses, the groups $C=C$ of the lignin, CO groups of cellulose, acetyl groups of lignin, CH groups and aromatic vibrations, CH_2 groups of polysaccharides. The Young's modulus of crystalline parts and non-crystalline parts evolves according to a linear law.

CONFLICT OF INTERESTS

The authors have not declared any conflict of interests.

REFERENCES

[1] De Assis S, Ranade R, Wunder SL, Mc Cool J, Borberick K, and Baran G (2004). Interface effects on mechanical properties of particle-reinforced composite, Dental Materials 20,677-686.DOI : 10.1016/j. dental. 2003.12.001.

[2] Zaman HU, Beg MDH (2016). Banana fiber strands-reinforced polymer matrix composites, Composites Interfaces:30,115DOI:10.1080/09276440.2016.1137178.

[3] Udoetok IAW, and Headley JV (2018). Ultra-Sonication Assisted Cross-Linking of Cellulose Polymers. Ultrasonics - Sonochemistry , 42, 567-576. https://doi.org/10.1016/j.ultsonch.2017.12.017.

[4] Kong D, and Wilson LD (2017). Synthesis and Characterization of Cellu- lose-Goethite Composites and Their Adsorption Properties with Roxarsone.CarbohydrPolym, 169, 282-294. https://doi.org/10.1016/j.carbpol.2017.04.019.

[5] Mahdyiar M, Galgana G, Shen-Tu B, Klein E, Pontbriand C W (2014). Formulation and Application of a Physically-Based Rupture Probability Model for Large Earthquakes on Subduction

Zones: A Case Study of Earthquakes on Nazca Plate. American Geophysical Union, Fall Meeting 2014. 2014AGUFM.S33E08M.

[6] Yeri Dah-T, Lamine Z, Mohamed S, Raguilnaba O (2018). Mechanical, Microstructural and Mineralogical Analyses of Porous Clay Pots Elaborated with Rice Husks. Journal of Minerals and Materials Characterization and Engineering, 6, 257-270.

[7] Asmak A, Harada H, Katayama Y, Nishikawa H, Mitoma Y, Tomoyuki M (2018). Phosphorus Adsorption and Nitric Acid Reduction by Ferrous Sulfate-Treated Foamed Waste Glass. Journal of Materials Science and Chemical Engineering .2327-6053.

[8] Yang Q, Wang XL, Luo W, Sun J, Xu QX, Chen F, Zhao JW, Wang S, Yao FB, Wang DB, Li XM, and Zeng GM (2018). Effectiveness and Mechan- isms of Phosphate Adsorption on Iron-Modified Biochars Derived from Waste Activated Sludge. Bioresource Technology, 247, 537-544. https://doi.org/10.1016/j.biortech.2017.09.136.

[9] Kazmina OV, Tokareva AY, and Vereshchagin VI (2016). Using Quartzo- feldspathic Waste to Obtain Foamed Glass Material. Resource - Efficient Technologies, 2, 23-29.

[10] Feng Xu, Yong-Cheng Shi, Donghai Wang (2013). X-ray scattering studies of lignocellulosic biomass, Accepted 9 February, Carbohydrate Polymers 94 (2013) 904– 917.

[11] Song XJ, Chen ZH, Wang XM, and Zhang SJ (2017). Ligand Effects on Nitrate Reduction by Zero-Valent Iron: Role of Surface Complexation. WaterResearch, 114, 218-227. https://doi.org/10.1016/j.watres.2017.02.040

[12] Taallah B, Guettala A. and Kriker A (2014). Effet de la teneur en fibres de palmier dattier et de la contrainte de compactage sur les propriétés des blocs de terre comprimée, Courrier du Savoir, N°18, 45-51. Analyse statistique et effet des traitements chimique sur le comportement physico-mécanique des fibres des bras de grappe des palmiers dattier. Rev. Sci. Technol., Synthèse 31 : 108 - 120.

[13] Su YM, Sun XY, Zhou XF, Dai CM and Zhang YL,. (2015) Zero-Valent Iron Doped Carbons Readily Developed from Sewage Sludge for Lead Removal from Aqueous Solution. Journal of Environmental Science, 36, 1-8. https://doi.org/10.1016/j.jes.2015.03.018.

[14] Jawad AH, Islam MA and Hameed BH (2017). Cross-Linked Chitosan Thin Film Coated onto Glassplate as an Effective Adsorbent for Adsorption of Reactive Orange 16. International Journal of Biological Macromolecules , 95, 743-749. https://doi.org/10.1016/j.ijbiomac.2016.11.087.

[15] Nguyen TAH, Ngo HH and Guo WS (2013). Feasibility of Iron Loaded "Oka- ra" for Biosorption of Phosphorous in Aqueous Solutions. Bioresource Technology , 150, 42-49. https://doi.org/10.1016/j.biortech.2013.09.133.

[16] Kubouchi M, Tumolva TP, Shimamura Y (2013). Biofiber-reinforced thermoset composites, in Polymer Composites (eds Thomas S, Joseph K, Malhotra SK, Goda K, Sreekala MS), Wiley-VCH Verlag GmbH & Co. KGaA, Weinheim, Germany. doi: 10.1002/9783527674220.ch6.

[17] Lunge S, Singh S, and Sinha A (2014). Magnetic Iron Oxide (Fe_3O_4) Nanoparticles from Tea Waste for Arsenic Removal. J. Magn. Magn. Mater. , 356. https://doi.org/10.1016/j.jmmm.2013.12.008.

[18] Nguong CW, Lee SNB, Sujan D (2013). A Review on Natural Fibre Reinforced Polymer Composites. Int. J. Chem. Nucl. Metallogr. Mater. Eng. 7(1):33-40.

[19] Liu K, Zhang X, Takagi H, Yang Z, & Wang D (2014). Effect of Chemical Treatments on Transverse Thermal Conductivity of Unidirectional Abaca Fiber/Epoxy Composite. Composites P a rt A : A p p li e d Science and Manufacturing , Vol 66, 227-236. [9] Sivam R., 2009. Potential of Brazilian.

[20] Christophe B (2013). Fibres naturelles de renfort pour matériaux composites. Éditions Techniques de l'Ingénieur • 249, rue de Crimée 75019 Paris–France.

[21] Burkill HM (1985). The useful plants of West Tropical Africa. 2nd Edition. Volume 1, Families A–D. Royal Botanic Gardens, Kew, Richmond, United Kingdom. 960 pp.

[22] Tra Bi FH, Kouamé FN, and Traoré D (2005). Utilisation of climbers in two forest reserves in West Côte d'Ivoire. In: Bongers, F., Parren, M.P.E. & Traoré, D. (Editors). Forest climbing plants of West Africa. Diversity, ecology and management. CABI Publishing, Wallingford, United Kingdom. pp. 167–181.

[23] Bosch CH (2018). PROTA Network Office Europe, Wageningen University, P.O. Box 341, 6700 AH Wageningen, Netherlands Consulté le 8 mars 2018.

[24] Ouajai S, Shanks RA (2005). Composition, structure and thermal degradation of hemp cellulose after chemical treatment. Polymer Degradation and Stability, v.89, p.327-335.

[25] Thygesen A, Oddershede J, Lilholt H, Thomsen A B, Stahl K (2005). On the determination of cristallinity and cellulose content in plant fibres. Cellulose, v.12, p.563-576.

[26] Cox HL (1952). The elasticity and strength of paper and other fibrous materials, British Journal of Applied Physics 55 72–79.

[27] Atangana J, Ebanda FB, Nnengue YS (2018). Morphological and Mechanical Characterizations of Neuropeltis Acuminata Fibers (NA). Publication in progress in the following journal: Journal of Chemical Engineering and Materials Science.

[28] Karine Charlet (2015). Contribution to the study of unidirectional composites reinforced by flax fibers: relation between the microstructure of the fiber and its mechanical properties, HAL Id: tel-01133091, https: //hal.archives-ouvertes.fr/tel-01133091.

[29] Chokouadeu Youmssi DV, Modtegue Bampel YD, Njankouo JM, Saha Tchinda JB (2017). Chemical composition of some plantation wood species (Eucalyptus saligna, Cupressus lusitanica and Eucalyptus paniculata) and assessment of compatibility with plaster. Journal of the Indian Academy of Wood Science ISSN 0972-172X Volume 14 Number 2. J Indian Acad Wood Sci 14:146-153 DOI 10.1007/s13196-017-0200-3.

[30] Tumolva TP, Vitoa JKR, Ragasaa JCR and Dela Cruza RMC (2017). Mechanical properties of natural fiber reinforced polymer (NFRP) composites using anahaw (Saribus rotundifolius) fibers treated with sodium alginate, Journal of Chemical Engineering and Materials Science, CD218FB66454.

[31] Igor Maria De Rosa A, Josè Maria Kenny B, Debora Puglia B, Carlo Santulli C, Fabrizio Sarasini (2009). Morphological Thermal and mechanical characterization of okra (Abelmoschus

esculentus) fibres as potential reinforcement in polymer composites. Composites Science and Technology xxx–xxx.

[32] Ntenga R (2007). Multi-scale modeling and characterization of the elastic anisotropy of plant fibers for the reinforcement of composite materials. Plant's biology. Blaise Pascal University - Clermont-Ferrand II; University of Yaoundé. French. <NNT: 2007CLF21759>. <Tel-00718126>

[33] Marta FV, Elias B, Christoph B, Alexander B, and Koon-Yang L (2017). Plant fibre-reinforced polymers: where do we stand in terms of tensile properties? International materials rewies, http://dx.doi.org/10.10.80/09506608.2016.1271089

[34] Adil Sbiai (2011). Composite materials with epoxy matrix loaded with date palm fibers: effect of tempo oxidation on fibers. Other. INSA Lyon. French. <NNT: 2011ISAL0043>,<Tel-00738814>.

[35] Alix S, Philippe E, Bessadok A, Lebrun L., Morvan C, Marais S (2009). Effect of chemical treatments on water sorption and mechanical properties of flax fibres.Bioresour.Technol. 100, 4742–4749.

[36] Haque MDM, Hasan M, Islam MDS, Ali MDE (2009). Physico-mechanical properties of chemically treated palm and coir fibre reinforced polypropylene composites. Bioresour.Technol. 100, 4903–4906.

[37] Sinha S, Rout SK (2008). Influence of fibre-surface treatment on structural, thermal and mechanical properties of jute. J. Mater. Sci. 43, 2590–2601.

[38] Helbert WJ, Sugiyma M, Ishihara S, Yamanaka (1997). Characterization of native crystalline cellulose in the cell walls of Oomycota, Journal of biotechnology, 57, 29-37, 1997.

[39] Segal L, Creely JJ, Martin AE, Conrad CM (1959). An empirical method for estimating the degree of crystallinity of native cellulose using the X-ray diffractometer. Textile Res. J., v.29, p. 786 - 794.

[40] Saito T, Okita Y, Nge TT, Sugiyama J, Isogai A (2006). Tempo-mediated oxidation of native cellulose: Microscopic analysis of fibrous fractions in the oxidized products. Carbohydrate Polymers, v.65, p.435-440.

[41] Sedan D (2007). Study of physicochemical interactions at hemp fiber / cement interfaces. Influence on the mechanical properties of the composite. Thesis of Faculty of Science and Technology, Limoges. Doctoral School Sciences - Technology - Health Study Group of Heterogeneous Materials N ° 63-2007.